The optimization of the dielectric layer photonic crystal filter by the quadratic response surface methodology

HONGWEI YANG[*], SHANSHAN MENG, GAIYE WANG, CUIYING HUANG

College of Applied Sciences, Beijing University of Technology,
Beijing 100124, China

[*]Corresponding author: yanghongwei@bjut.edu.cn

Dielectric layer photonic crystal filter structures in waveguide are optimized by the quadratic response surface methodology. The optimization model of the filter is established on the basis of the analysis which is conducted with the aid of the response surface methodology. The model is solved using sequential quadratic programming and the optimal parameters are obtained. Examples demonstrate it is effective.

Keywords: optimization, photonic crystal filter, response surface methodology.

1. Introduction

Photonic crystals are periodic arrays of dielectric composites that exhibit photonic band gaps. The electromagnetic waves in a certain frequency range cannot propagate in photonic crystals [1]. Due to the stop-band property of photonic crystals, they have attracted considerable scientific interests in the design of this filter during the past decades [2]. The dielectric layer photonic crystal structures in waveguide were originally developed in optical frequencies, and they are scalable to microwave and millimetre -wave frequencies [3, 4]. In this paper, the optimal design of a dielectric layer photonic crystal filter using the response surface methodology (RSM) is described.

In the design of a one-dimensional photonic crystal filter, the common optimization methods are the following: simulated annealing (SA) [5], genetic algorithm (GA) [6], particle swarm optimization (PSO) and so on. SA can solve the problem of a local minimum value in the computation process, but the time consumption increases exponentially with an increase in the number of variables and this method is always used for a simple system analysis [7]. Both GA and PSO are similar in a sense that these two techniques are population-based search methods and they search for the optimal solu-

tion by updating generations [8]. However, GA has complex evolution operators such as crossover and mutation, and the convergence is slow when approaching the optimum. Compared to GA, the advantages of PSO are that PSO is easy to implement and has few parameters to adjust, but it has no system of analysis methods and mathematical basis, and an application range is small [9].

The RSM stemmed from experimental design and was later introduced into numerical simulations in reliability assessment of complex multivariable systems [10, 11]. The basic idea of RSM is to approximate the actual state function, which may be implicit and/or very time-consuming to evaluate, with the so-called response surface function that is easier to apply to the complex problem, and the response surfaces generally take a quadratic form. For further reading about the RSM, see [12]. In contrast with other optimization methods, RSM is mainly used for statistical model building and location of maxima. To construct an approximate model with RSM, no sensitivity analysis was required, thus it is applicable for problems with sensitivity difficulty. Response surface construction involved no information inside the structural analysis procedure, hence it can be applied to a variety of problems and their mixture.

In this paper, the optimization model of the filter is established first. Then it is dealt with RSM. At last, the model is solved by using sequence quadratic programming and the optimal parameters are obtained. Examples show its precision and efficiency.

2. Bring forward the control model

Dielectric layer photonic crystal filter structure in waveguide is shown in Fig. 1. It is a periodic dielectric structure designed to have photonic band gaps. The periodic length is a, the dielectric thickness is d and the relative permittivity of the dielectric is ε_r. They are the three major factors in determining the stop-band characteristics of the waveguide dielectric layer photonic crystal structures [13]. In this study we aim at optimizing a, d and ε_r to control the stop-band characteristics of the dielectric layer photonic crystal filter.
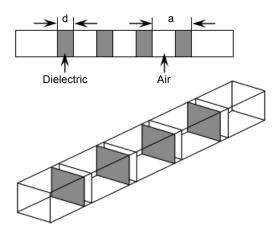

Fig. 1. A model of dielectric layer photonic crystal filter structure in a waveguide.

Because the waveguide dielectric layer photonic crystal structure has a stop-band characteristics, it can be used as a stop-band filter. The smaller is the transmission co-efficient in a stop-band is and the larger transmission coefficient beyond a stop-band is, the better are the properties of the filter. When the width of the stop-band is fixed, we hope the area surrounded by the transmission coefficient curve and horizontal axis (frequency axis) should be maximum. Thus the control model is established as:

$$
\begin{cases}
\text{Find:} & a, d, \varepsilon_r \\[2mm]
\text{Maximum:} & A_{sb} = \int_{f_2}^{f_3} (-S_{21}) \mathrm{d}f \\[2mm]
\text{Subject to:} & \underline{a} \le a \le \overline{a} \\[2mm]
\text{Subject to:} & \underline{d} \le d \le \overline{d} \\[1mm]
& d \le ka \\[2mm]
& \underline{\varepsilon_r} \le \varepsilon_r \le \overline{\varepsilon_r} \\[2mm]
& A_L = \int_{f_1}^{f_2} (-S_{21}) \mathrm{d}f \le T_L \\[2mm]
& A_R = \int_{f_3}^{f_4} (-S_{21}) \mathrm{d}f \le T_R
\end{cases}
\tag{1}
$$

where the periodic length a, dielectric thickness d, relative permittivity ε_r of the dielectric are the design variables; f_2 and f_3 are the lower and upper bound of the stop-band, f_1 is the lower bound of the concerned band on the left of the stop-band, f_4 is the upper bound of the concerned band on the right of the stop-band. Define A_{sb} as a negative of transmission quantity at the region between f_2 and f_3. The larger is A_{sb}, the smaller transmission quantity is. Similarly, A_L and A_R are negatives of transmission quantities at corresponding regions. Parameters T_L and T_R are permitted maximum of transmission quantity negative at corresponding regions. Parameters $\underline{a}$, $\overline{a}$, $\underline{d}$, $\overline{d}$, $\underline{\varepsilon_r}$, $\overline{\varepsilon_r}$ are the lower and upper bound of the design variables (a, d, ε_r), respectively. Parameter k is a positive number less than 1 because d is less than a.

Due to a strong nonlinear characteristics of the problem, it is very difficult to deduce an explicit expression of the objective function A_{sb} with design variables a, d and ε_r. Fortunately, we can modify the original function Eq. (1) to an approximate one and make the optimization based on the approximate expression. In this study, such approximation was carried out by the RSM.

3. Response surface methodology

3.1. Function fitting

For the objective function, the response surface generally takes a quadratic polynomials form. Higher order polynomials generally are not used for a conceptual reason as well as for a computational one. In this paper, we use a quadratic form containing

the crossing terms. Considering the full quadratic polynomial form, the response estimated equation for three variable designing is given by:

$$\tilde{y} = \beta_0 + \beta_1 x_1 + \beta_2 x_2 + \beta_3 x_3 + \beta_4 x_1^2 + \beta_5 x_2^2 + \beta_6 x_3^2 +$$
$$+ \beta_7 x_1 x_2 + \beta_8 x_1 x_3 + \beta_9 x_2 x_3 \tag{2}$$

where $\beta_0, \beta_1, ..., \beta_9$ are 10 coefficients to be determined, and x_1, x_2, x_3 represent a, d and ε_r, respectively in this paper.

In order to determine all betas, we should select m ($m \geq 10$) experimental points. Putting the coordinates of m experimental points into Eq. (2), we can get m estimated response values

$$\tilde{y}_i = \beta_0 + \beta_1 x_{i1} + \beta_2 x_{i2} + \beta_3 x_{i3} + \beta_4 x_{i1}^2 + \beta_5 x_{i2}^2 + \beta_6 x_{i3}^2 +$$
$$+ \beta_7 x_{i1} x_{i2} + \beta_8 x_{i1} x_{i3} + \beta_9 x_{i2} x_{i3}, \qquad i = 1, ..., m \tag{3}$$

where x_{i1}, x_{i2} and x_{i3} represent a, d and ε_r of the i-th experimental point, respectively.

In fact, we can also get actual values of m experimental points, represented by y_i ($i = 1, ..., m$).

Define error $\varepsilon = (\varepsilon_1, \varepsilon_2, ..., \varepsilon_m)^T$ between the actual and the estimated responses,

$$\varepsilon_i = \tilde{y}_i - y_i, \qquad i = 1, ..., m \tag{4}$$

Using the least square technique, and minimizing the residual error measured by the sum of square deviations between the actual and the estimated responses, we have

$$S = \sum_{i=1}^{m} \varepsilon_i^2 = \sum_{i=1}^{m} (\tilde{y}_i - y_i)^2 \rightarrow \min \tag{5}$$

Let

$$\frac{\partial S}{\partial \beta_j} = 0, \qquad j = 1, ..., 9 \tag{6}$$

Equation (6) is a system of 10 linear equations with 10 unknowns. Solving Eq. (6), we can find all betas and obtain the quadratic response function:

$$y = \beta_0 + \beta_1 x_1 + \beta_2 x_2 + \beta_3 x_3 + \beta_4 x_1^2 + \beta_5 x_2^2 + \beta_6 x_3^2 +$$
$$+ \beta_7 x_1 x_2 + \beta_8 x_1 x_3 + \beta_9 x_2 x_3 \tag{7}$$

Equation (7) is the actual quadratic response function and $\beta_0, \beta_1, ..., \beta_9$ are determined.

3.2. Move limits and normalized variables

The sequential quadratic programming is used to obtain the optimum. In the optimization process, suppose $x_l^{(v)}$ ($l = 1, 2, 3$) is the present designed point of l-th variable

in *v*-th iteration, and specify artificially a step size $\Delta_l^{(v)}$ for *l*-th variable. The expression of move limits is

$$\begin{cases} \underline{x}_l^{(v)} = x_l^{(v)} + \Delta_l^{(v)} \\ \bar{x}_l^{(v)} = x_l^{(v)} - \Delta_l^{(v)} \end{cases}, \quad l = 1, 2, 3 \tag{8}$$

where $\underline{x}_l^{(v)}$ and $\bar{x}_l^{(v)}$ represent the upper and lower bound, respectively. The interval of *l*-th designed variable x_l is $[\underline{x}_l^{(v)}, \bar{x}_l^{(v)}]$ in *v*-th iteration.

Furthermore, to improve numerical stability, it is a good practice to scale all variables so that each variable changes in the range $[-1, 1]$ [14]. Let $\zeta_l, l = 1, 2, 3$, represent the normalized variables. The transformation formula is as follows [15]:

$$\zeta_l = \frac{2x_l - (\bar{x}_l + x)}{\bar{x}_l - x_l} \quad l = 1, 2, 3 \tag{9}$$

After the optimization, we can return to initial design variables and get their value by the following transformation:

$$x_l = \frac{(\bar{x}_l - \underline{x}_l)\zeta_l}{2} + \frac{\bar{x}_l + \underline{x}_l}{2} \quad l = 1, 2, 3 \tag{10}$$

3.3. The selection of experimental points

How to select the experimental points? The selection of points in the designing space where the response should be evaluated is commonly called the design of experiments. The choice of the experimental design can have a large influence on the accuracy of the approximation and the cost of constructing the response surface. For quadratic response models, the central composite design (CCD) is an attractive alternative [16]. There are 15 experimental points in CCD method for three designing variables, where 8 points are at vertices of a quadrilateral, 6 are along the three symmetry axis, and one
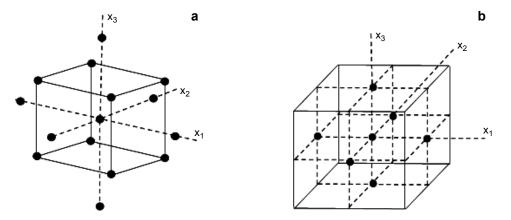

Fig. 2. Design of experiments for objective (**a**) and constraint (**b**) response surface.

is at the centre. Figure 2**a** shows an example of CCD for the objective response surface. In the paper, this method is used to choose the experimental design. This means that 15 experiment points ($m = 15$) are chosen to determine the value of betas. After three designed variables are normalized, in terms of the coordinates the corners of the cube are $(-1, -1, -1)$, $(1, -1, -1)$, $(1, 1, -1)$, $(-1, 1, -1)$, $(-1, -1, 1)$, $(1, -1, 1)$, $(1, 1, 1)$, $(-1, 1, 1)$; the centre point is $(0, 0, 0)$. According to [10], the distance between the axial point and the centre point is 1.215, so the axial points are at $(-1.215, 0, 0)$, $(1.215, 0, 0)$, $(0, -1.215, 0)$, $(0, 1.215, 0)$, $(0, 0, -1.215)$, $(0, 0, 1.215)$.

For constraint functions, the response surfaces are constructed at the same value of the selected designing parameters. In this paper, the number of the selection of points for the constraint response is 7 for three variables. Of which, 6 are symmetrical distribution on the axis and one is at the centre. Figure 2**b** shows an example of design of experiments for the constraint response surface.

4. The control model used for solving

First, change the maximum problem into an objective minimization problem. Let the new objective function

$$G = -A_{sb} \tag{11}$$

Then, based on the above discussion, the control model is converted into a sequential quadratic programming problem. It is stated as:

$$
\left\{
\begin{array}{ll}
\text{Find:} & a, d, \varepsilon_r \\[2mm]
\text{Minimize:} & G = \dfrac{x^T H x}{2} + g^T x \\[2mm]
\text{Subject to:} & \underline{x}_1^{(v)} \le a \le \bar{x}_1^{(v)} \\[2mm]
& \underline{x}_2^{(v)} \le d \le \bar{x}_2^{(v)} \\[2mm]
& d/a \le k \\[2mm]
& \underline{x}_3^{(v)} \le \varepsilon_r \le \bar{x}_3^{(v)} \\[2mm]
& A_L^T x + B_L \le T_L \\[2mm]
& A_R^T x + B_R \le T_R
\end{array}
\right. \tag{12}
$$

where $x = (a, d, \varepsilon_r)^T, H, g, A_L, B_L, A_R, B_R$ are obtained by RSM to deal with the objective function and the constraint functions, Eq. (12) is a standard quadratic programming problem. The sequential quadratic programming is used to solve the model.

5. Numerical results

Numerical example 1: design a dielectric layer photonic crystal filter as shown in Fig. 1. The centre frequency stop-band of the filter is 6 GHz and the bandwidth of the filter is 2 GHz. The width and height of the waveguide are 57 and 23 mm, respectively. Let the number of waveguide period be 9 and $f_1 = 3$ GHz, $f_2 = 5$ GHz, $f_3 = 7$ GHz, $f_4 = 9$ GHz, $T_L = T_R = 2.5$, $\underline{a} = 0.002$ mm, $\overline{a} = 100$ mm, $\underline{d} = 0.001$ mm, $\overline{d} = 100$ mm, $\underline{\varepsilon_r} = 1.1$, $\overline{\varepsilon_r} = 10$, and $k = 0.9$. The initial design variables are $a = 20$ mm, $d = 15$ mm and $\overline{\varepsilon_r} = 2.25$.

Figure 3**a** gives a curve of the objective function varying with the iteration number obtained by RSM. It is clearly seen that, at the beginning, the value of the objective function G decreases rapidly, and after 8 iterations the value obtained by RSM keeps constant at about –62 dB·s. With the RSM, we obtain a, d and ε_r which are 22.2 mm, 6.7 mm and 2.8, respectively, after 16 iterations. Figure 3**b** gives the curves of the de-
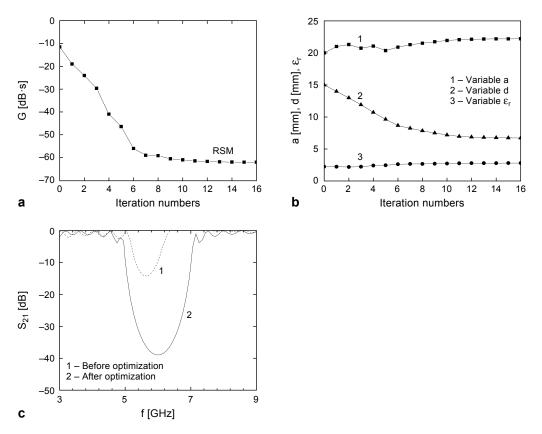

Fig. 3. The optimization process and results for example 1. Object function *versus* iteration number (**a**). Design variables *versus* iteration numbers (**b**). Stop-band characteristics before optimization and after optimization (**c**).

sign variable *versus* iteration numbers. From Figs. 3**a** and 3**b** we can see that the optimization process is convergent. Stop-band characteristics before optimization and after optimization are given in Fig. 3**c**. It is obvious that, before optimization, the stop-band is not deep and wide, and the minimization of the transmission coefficient is –14.3 dB. After optimization, the centre frequency stop-band of this filter is 6 GHz and the width of band is 2 GHz, the minimum of the transmission coefficient is nearly –38.9 dB, the depth of the stop-band is over two times deeper that the non-optimized stop-band. The optimal design is carried out.

Numerical example 2: as in the case of example 1, the stop-band centre frequency of the filter is designed at 6 GHz and the width of the band is 2 GHz. All data in these two examples are the same except the initial design variables. Here we choose the initial design variables at $a = 25$ mm, $d = 12$ mm and $\varepsilon_r = 1.5$.

Figures 4**a** and 4**b** give the curves of the objective function and the design variables varying with the iteration number respectively. We can get from Figs. 4**a** and 4**b** that the objective functional value is convergent at about –62 dB·s, and after 20 iterations a, d and ε_r are about 22.2 mm, 6.7 mm and 2.8, respectively. The optimal result is con-
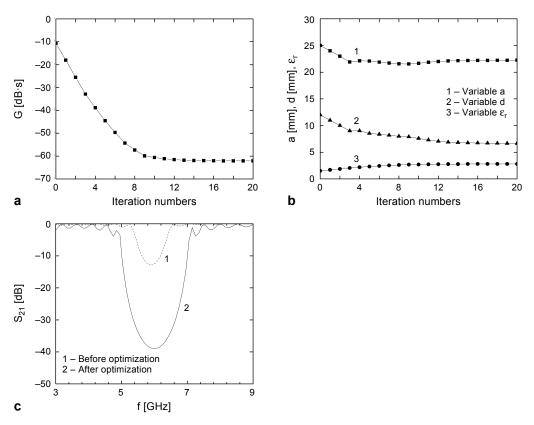

Fig. 4. The optimization process and results for example 2. Object function *versus* iteration number (**a**). Design variables *versus* iteration numbers (**b**). Stop-band characteristics before optimization and after optimization (**c**).

sistent with the result of example 1, which demonstrates that the optimization process is independent of the initial design variables and the method in this paper is stable. Stop-band characteristics before optimization and after optimization are given in Fig. 4**c**. We can get from Fig. 4**c** that the stop-band centre frequency of this filter is 6 GHz before optimization, but the stop-band is not deep and wide. Similarly, the centre frequency is still 6 GHz after optimization, but the stop-band is deep and the width of band is 2 GHz, which achieves the desired objectives.

Numerical example 3: change the bandwidth of the filter in above two examples. The centre frequency stop-band of this filter is designed at 6 GHz and the width of band is 1.4 GHz. The dimension of the waveguide is the same as the one in these examples. Let $f_1 = 3.3$ GHz, $f_2 = 5.3$ GHz, $f_3 = 6.7$ GHz, $f_4 = 8.7$ GHz, $T_L = T_R = 1$, $\underline{a} = 0.002$ mm, $\overline{a} = 100$ mm, $\underline{d} = 0.001$ mm, $\overline{d} = 100$ mm, $\underline{\varepsilon_r} = 1.1$, $\overline{\varepsilon_r} = 10$, and $k = 0.9$. The initial design variables are $a = 20$ mm, $d = 15$ mm and $\varepsilon_r = 2.25$.

Figures 5**a** and 5**b** give the optimization process and result of 20 iterations. After 20 iterations, the objective functional value keeps constant at about -21.5 dB·s, where a, d and ε_r are about 23.8 mm, 9.0 mm and 1.8, respectively. Stop-band characteristics
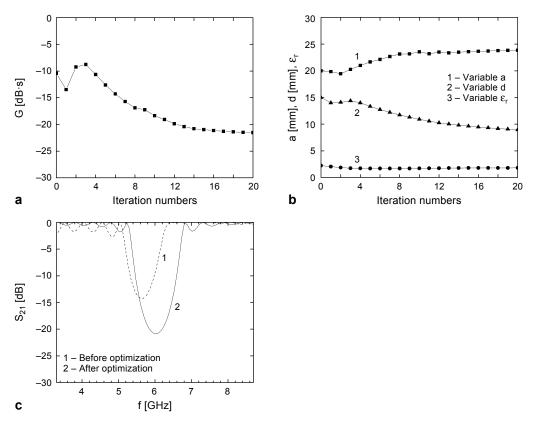

Fig. 5. The optimization process and results for example 3. Object function *versus* iteration number (**a**). Design variables *versus* iteration numbers (**b**). Stop-band characteristics before optimization and after optimization (**c**).

before optimization and after optimization are given in Fig. 5**c**. Figure 5**c** shows that the centre frequency stop-band of this filter is 6 GHz and the width of band is 1.4 GHz, indicating that the optimization process is effective. We can use RSM to design dielectric layer photonic crystal filters with different bandwidth and centre frequency stop-band. If the dielectric material is determined in practical applications, *i.e*, the dielectric constant ε_r is known, we just need to optimize periodic length *a* and dielectric thickness *d*. However, in this paper all the three design variables are optimized by RSM, and the suitable dielectric material and dimension for assembling the filter can be selected according to the optimization results.

6. Conclusion

The RSM was first used to optimize the dielectric layer photonic crystal filter structures in waveguide. The objective function is transmission quantity. After the optimization, the value of the objective function is much less than that before the optimization. The optimization results demonstrate that: 1) Due to the fact that no sensitivity analysis is required, we can apply RSM to optimize the dielectric layer photonic crystal filter. 2) The optimization process is convergent, which is obviously shown in Figs. 3**a** and 3**b**. 3) The numerical example 2 shows that the optimization process is independent of the initial design variables, indicating that RSM is a stable algorithm for filter optimization. 4) It is clearly seen in Figs. 3**c**, 4**c** and 5**c** that the depth and the width of the optimized stop-band is significantly improved, especially that it is over two times deeper that the non-optimized stop-band in Figs. 3**c** and 4**c**, denoting the effectiveness of this method. The optimal filter that satisfies the centre frequency and stop-band width requirements can be designed by RSM.

References

[1] He Jie, Song Li-tao, Wang Hua-lei, Han Yi-ang, Li Tao, *Polarization sensitive performance of one dimensional photonic crystal filters with a liquid crystal layer*, Optoelectronics Letters **6**(6), 2010, pp. 432–434.

[2] Haixia Qiang, Liyong Jiang, Wei Jia, Xiangyin Li, *Design of one-dimensional dielectric and magnetic photonic crystal filters with broad omnidirectional filtering band*, Optica Applicata **41**(1), 2011, pp. 63–77.

[3] Rumsey I., Piket-May M., Kelly P.K., *Photonic bandgap structures used as filters in microstrip circuits*, IEEE Microwave and Guided Wave Letters **8**(10), 1998, pp. 336–338.

[4] Iluz Z., Shavit R., Bauer R., *Microstrip antenna phased array with electromagnetic bandgap substrate*, IEEE Transactions on Antennas and Propagation **52**(6), 2004, pp. 1446–1453.

[5] Zhao Xing-Xing, Zhu Qiao-Fen, Zhang Yan, *The design of a photonic crystal filter in the terahertz range*, Chinese Physics B **18**(7), 2009, pp. 2864–2867.

[6] Jiandong Mao, Juan Li, Chunyan Zhou, Hu Zhao, Hongjiang Sheng, *Optimum design of a photonic crystal filter based on a genetic algorithm used in a rotational Raman lidar*, Laser Physics **23**(2), 2013, article 026003.

[7] Lv X.Y., *The Reseach in Application of the Photonoc Crystal Filter*, Master Thesis, Xinjiang University, 2006, (in Chinese).

[8] Djavid M., Mirtaheri S.A., Abrishamian M.S., *Photonic crystal notch-filter design using particle swarm optimization theory and finite-difference time-domain analysis*, Journal of the Optical Society of America B **26**(4), 2009, pp. 849–853.

[9] Lei K.Y., *The Reseach in Application of Particle Swarm Optimization Algorithm*, Doctor Thesis, Southwest University, 2006, (in Chinese).

[10] Roux W.J., Stander N., Haftka R.T., *Response surface approximations for structural optimization*, International Journal for Numerical Methods in Engineering **42**(3), 1998, pp. 517–534.

[11] Jansson T., Nilsson L., Redhe M., *Using surrogate models and response surfaces in structural optimization – with application to crashworthiness design and sheet metal forming*, Structural and Multidisciplinary Optimization **25**(2), 2003, pp. 129–140.

[12] Ren L.Q., *Experimental Optimization Technology*, China Machine Press, 1987, pp. 147–154.

[13] Yan Dun-bao, Yuan Nai-chang, Fu Yun-qi, *Research on dielectric layer PBG structures in wave-guide based on FDTD*, Journal of Electronics and Information Technology **26**(1), 2004, pp. 118–123.

[14] Huiping Yu, Yunkan Sui, Jing Wang, Fengyi Zhang, Xiaolin Dai, *Optimal control of oxygen concentration in a magnetic Czochralski crystal growth by response surface methodology*, Journal of Materials Science and Technology **22**(2), 2006, pp. 173–178.

[15] Yunkang Sui, Huiping Yu, *The Improvement of Response Surface Method and the Application of Engineering Optimization*, Science Press, 2010, pp. 11–32.

[16] Vitali R., *Response Surface Method for High Dimensional Structural Design Problem*, Ph.D. Thesis, University of Florida, 2000.